Dyes and Pigments 91 (2011) 495–500

Contents lists available at ScienceDirect

Dyes and Pigments

journal homepage: www.elsevier.com/locate/dyepig

Single-layer white polymer light-emitting diodes based on an iridium (III) complex containing alkyltrifluorene picolinic acid

Yafei Wang [a], Yu Liu [a,*], Zhiyong Zhang [a], Jian Luo [a], Danyan Shi [a], Hua Tan [a], Gangtie Lei [a], Meixiang Zhu [a], Weiguo Zhu [a,*], Yong Cao [b,**]

[a] College of Chemistry, Key Lab of Environment-Friendly Chemistry and Application of the Ministry of Education, Xiangtan University, Xiangtan 411105, China
[b] Institute of Polymer Optoelectronic Material and Devices, South China University of Technology, Guangzhou 510640, China

ARTICLE INFO

Article history:
Received 24 February 2011
Received in revised form
20 April 2011
Accepted 20 April 2011
Available online 23 April 2011

Keywords:
Fluorene
Iridium (III) complex
Phosphorescence
White polymer light-emitting devices
Exciplex emission
Electron injection

ABSTRACT

To explore the relationship between the electronic properties of a host/dopant system and obtain a high-efficiency single-dopant white polymer light-emitting device two novel blue-emitting cyclometalated iridium (III) complexes of $(dfppy)_2Ir(Tfl\text{-}pic)$ and $(dfppy)_2Ir(Brfl\text{-}pic)$ have been synthesized and characterized, where dfppy is 2-(2,4-difluorophenyl)pyridine, Tfl-pic and Brfl-pic are picolinic acid derivatives containing trialkylfluorene and dibromoalkylfluorene units bridged with an alkoxy chain, respectively. Both iridium (III) complexes exhibited blue emission in dichloromethane solution and their neat films, and possessed good dispersibility and thermal properties. Two different devices using $(dfppy)_2Ir(Tfl\text{-}pic)$ as a single component emitter and a blend of poly(*N*-vinylcarbazole) and 2-(4-biphenyl)-5-(4-*tert*-butylphenyl)-1,3,4-oxadiazole as the host matrix were fabricated. Improved white emission was obtained by adjusting the electron injection layer leading to efficient exciplex emission.

1. Introduction

White organic light-emitting diodes (WOLEDs) are of growing interest for the next generation of displays and solid-state lighting technologies owing to their low-cost, high-efficiency and flexible properties [1–7]. Among the reported WOLEDs, some fluorescent [8–11] or phosphorescent materials [12–15] are used as emitters in the emitting layer. Compared to fluorescent materials, phosphorescent materials exhibit high luminescent efficiency as they can harvest single and triplet excitons leading to 100% internal quantum efficiency in theory [16,17]. Therefore, Os^{II}- [18], Ir^{III}- [13,15] and Pt^{II}- [14,19] based heavy transition metal complexes have been significantly developed for wide application in WOLEDs. Among these organometallic phosphors, iridium (III) complexes have become the most promising candidates for WOLEDs owing to their good stability, high photoluminescence (PL) quantum yields, short triplet state lifetimes and non-planar configuration.

To date, most of the WOLEDs based on iridium (III) complexes have a multiple-emissive-layer (MEL) structure [20–22] and a single-emissive-layer (SEL) structure with multi-emitters [23]. For example, Thompson and Forrest et al. made an eight-layer WOLEDs with a power efficiency of 24 lm W^{-1} and an external quantum efficiency of 18%, which harvested singlet excitons from the blue-emitting fluorescent material and triplet excitons from both red-emitting $(piq)_2Ir(acac)$ and green-emitting $Ir(ppy)_3$ complexes, respectively [21]. Eom et al. recently reported another class of WOLEDs with a p-i-n structure comprising two adjacent emissive layers co-doped with three phosphorescent emitters of iridium (III) complex (red, green, and blue) [22]. Ma and co-workers co-doped blue-emitting and orange-emitting iridium (III) complexes into a host of 4,4′,4″-tris(*N*-carbazolyl)triphenylamine (TCTA) to achieve a type of SEL-based WOLEDs [23]. At the same time, some polymer derivatives with an iridium (III) complex chromophore have also been investigated in white polymer light-emitting diodes (WPLEDs) by Slugovc and Cao et al. [24,25]. To the best of our knowledge, there is no report on WPLEDs with a SEL structure utilizing a blue-emitting iridium (III) complex as a single doping emitter.

In our previously work [26], we reported that an iridium (III) complex containing an alkylfluorene-based picolinic acid derivative exhibited a significantly red-shifted emission in both its neat film

* Corresponding authors. Tel.: +86 731 58298280; fax: +86 731 58292251.
** Corresponding author. Tel.: +86 20 87114635.
E-mail addresses: liuyu03b@126.com (Y. Liu), zhuwg18@126.com (W. Zhu), poycao@scut.edu.cn (Y. Cao).

0143-7208/$ – see front matter © 2011 Elsevier Ltd. All rights reserved.
doi:10.1016/j.dyepig.2011.04.013

and polymer light-emitting diodes (PLEDs). In this regard, we expect this class of iridium (III) complexes with the same alkylfluorene-based picolinic acid derivative can achieve white emission in SEL-based PLEDs used as a single doping emitter if we tune the cyclometalated ligand structure. Therefore, we use the alkylfluorene-based picolinic acid derivatives of Tfl-picH and Brfl-picH [26] as the ancillary ligand and 2,4-difluorophenylpyridine (dfppy) instead of 1-phenyliso-quinoline as the cyclometalated ligand to design a class of blue-emitting iridium (III) complexes of $(dfppy)_2Ir$(Tfl-pic) and $(dfppy)_2Ir$(Brfl-pic) where Tfl-picH ligand is 6-(6′-(9″-octyl-2″,7″-bi(9, 9-dioctylfluoren-2-yl)fluoren-9″-yl)hexyloxy)picolinic acid and Brfl-picH ligand is 6-(6′-(2″,7″-dibromo-9″-octylfluoren-9″-yl)hexyloxy)picolinic acid. Their thermal, dispersible, electrochemical, optophysical and electroluminescent properties were investigated. White emission was obtained in the SEL-based PLEDs with a single dopant of $(dfppy)_2Ir$(Tfl-pic) and a cathode of LiF/Al.

2. Experimental section

2.1. Materials and equipment

All reagents were purchased from Aldrich, Acros or TCI companies. All reactions and manipulations were carried out under an inert gas atmosphere. ^{1}H NMR spectra were measured in $CDCl_3$ solution on a Bruker DPX (400 MHz) NMR spectrometer using tetramethylsilane(TMS) as the internal standard. Cyclic voltammograms (CV) were performed with a three electrode electrochemical cell in a 0.1 M tetra(*n*-butyl)-ammonium hexafluoro phosphate ($TBAPF_6$) solution in acetonitrile with a scan 100 mV s^{-1} at room temperature under argon atmosphere. A platinum wire and a KCl saturated Hg/HgO were used as counter electrode and reference electrode, respectively. A microplatinum ($\varnothing = 0.8$ mm) was used as the working electrode.

PLEDs were fabricated according to the reported procedures [27]. The devices have the following structures: i) ITO/PEDOT:PSS (50 nm)/iridium (III) complexes + PVK–PBD (45 nm)/Ca (4 nm)/Al (150 nm), ii) ITO/PEDOT:PSS (50 nm)/iridium (III) complexes + PVK–PBD (45 nm)/LiF (4 nm)/Al (150 nm), in which PEDOT:PSS is poly(3,4-ethylenedioxythiophene)/poly(styrenesulfonate), PVK is poly(*N*-vinylcarbazole) and PBD is 2-(4-biphenyl)-5-(4-*tert*-butylphenyl)-1,3,4-oxadiazole. ITO is used as the anode, PEDOT:PSS is used as a hole-injection layer and Ca/Al or LiF/Al is employed as a cathode. PBD weight ratio is 30 wt% in the PVK–PBD blend. The doping concentrations for the iridium (III) complex were from 1 wt% to 8 wt%.

2.2. Synthesis of $(dfppy)_2Ir$(Brfl-pic)

To a mixture of $IrCl_3 \cdot 3H_2O$ (0.3 g, 0.85 mmol) and water (5 mL) was added 2-(2,4-difluorophenyl)pyridine (0.5 g, 2.62 mmol) and 2-ethoxyethanol (15 mL). The mixture was heated under reflux under an inert gas atmosphere for 20 h. After cooled to temperature, the colored precipitate was filtered off and was washed with water, followed by hexane. The resulting dimer of $[(dfppy)_2IrCl]_2$ was obtained as a yellow solid (0.35 g, 67.7%).

A mixture of the foregoing dimer of $[(dfppy)_2IrCl]_2$ (0.15 g, 0.12 mmol), compound **Brfl-picH** (0.2 g, 0.31 mmol) and Na_2CO_3 (131 mg) was heated under reflux under an inert gas atmosphere in 2-ethoxyethanol (15 mL) for 12–15 h. After cooled to room temperature, the mixture was extracted with dichloromethane (DCM) and the combined organic layer was dried over anhydrous magnesium sulfate. The crude product was purified by dry flash silica gel column with petroleum ether (PE)/ethyl acetate (EA) (2:1–0:1) as eluent to gain the target product (0.24 g, 79.2%) as a yellow solid. ^{1}H NMR (400 MHz, $CDCl_3$, TMS), δ (ppm): 8.64 (d, $J = 4.88$ Hz, 1H), 8.26 (d, $J = 8.7$ Hz, 1H), 8.08 (d, $J = 8.9$ Hz, 1H), 7.99 (d, $J = 6.9$ Hz, 1H), 7.89 (t, 1H), 7.74 (t, 1H), 7.66 (t, 1H), 7.57 (t, 3H), 7.50–7.43 (m, 4H), 7.11 (t, 1H), 6.89 (t, 1H), 6.77 (d, $J = 8.4$ Hz, 1H), 6.39 (t, 1H), 6.21 (t, 1H), 5.65 (t, 1H), 5.41 (t, 1H), 3.56 (t, 2H), 1.92 (t, 4H), 1.25–0.75 (m, 20H), 0.59–0.48 (m, 3H). ^{13}C NMR (100 MHz, $CDCl_3$, TMS), δ (ppm): 173.27, 165.43, 164.06, 159.65, 154.24, 152.40, 151.26, 148.92, 148.24, 141.52, 139,15, 137.93, 137.85, 130.31, 126.17, 123.32, 123.12, 122.34, 122.15, 121.67, 121.56, 121.26, 121.04, 114.07, 109.50, 98.01, 95.97, 69.53, 55.65, 40.35, 40.09, 31.76, 29.93, 29.84, 29.48, 29.16, 27.46, 25.48, 23.70, 23.60, 22.60, 14.06. Anal. Calcd. for $C_{55}H_{50}Br_2F_4IrN_3O_3$: C 53.75, H 4.10, N 3.42. Found: C 53.51, H 4.20, N 3.38%.

2.3. Synthesis of $(dfppy)_2Ir$(Tfl-pic)

This compound was prepared according to the synthetic procedure described for $(dfppy)_2Ir$(Brfl-pic). A yellow solid was obtained with a yield of 78.2%. ^{1}H NMR (400 MHz, $CDCl_3$, TMS) δ (ppm): 8.59 (d, $J = 6.4$ Hz, 1H), 8.17 (d, $J = 7.2$ Hz, 1H), 8.07 (d, $J = 7.6$ Hz, 1H), 7.96 (d, $J = 7.6$ Hz, 1H), 7.86–7.52 (m, 18H), 7.36 (t, 6H), 7.06 (t, 1H), 6.83 (t, 1H), 6.69 (d, $J = 7.6$ Hz, 1H), 6.34 (t, 1H), 6.20 (t, 1H), 5.62 (d, $J = 9.2$ Hz, 1H), 5.38 (d, $J = 6.8$ Hz, 1H), 3.53 (t, 2H), 2.12–2.03 (m, 12H), 1.18–1.06 (m, 68H), 0.81–0.71 (m, 15H). ^{13}C NMR (100 MHz, $CDCl_3$, TMS), δ (ppm): 173.30, 165.35, 164.03, 154.26, 151.63, 151.58, 151.20, 150.99, 150.59, 148.89, 148.19, 141.47, 140.71, 140.68, 140.62, 140.50, 140.35, 140.30, 140.06, 137.86, 127.12, 126.87, 126.29, 126.0, 123.30, 123.01, 122.11, 121.64, 121.41, 121.34, 121.0, 120.04, 119.92, 119.77, 114.07, 113.70, 109.47, 98.02, 95.98, 69.55, 55.32, 55.22, 55.43, 40.64, 40.36, 31.79, 30.03, 29.72, 29.21, 27.54, 25.55, 24.03, 23.87, 22.60, 14.07. Anal. Calcd. for $C_{113}H_{132}F_4IrN_3O_3$: C 73.42, H 7.20, N 2.27. Found: C 72.91, H 7.20, N 2.26%.

3. Results and discussion

3.1. Syntheses and characterization

The synthetic route used to access the two iridium (III) complexes is shown in Scheme 1. Ancillary ligands of Brfl-pic and Tfl-pic were prepared according to our reported procedures [26]. The iridium (III) complexes $(dfppy)_2Ir$(Brfl-pic) and $(dfppy)_2Ir$(Tfl-pic) were obtained by a chloride cleavage of the $[(dfppy)_2IrCl]_2$ dimer with the ancillary ligands in a moderate yield. These iridium (III) complexes were characterized by NMR spectroscopy and elemental analysis.

3.2. Optophysical properties

Fig. 1 shows the UV/vis absorption and photoluminescence (PL) spectra of the $(dfppy)_2Ir$(Brfl-pic) and $(dfppy)_2Ir$(Tfl-pic) complexes in DCM at room temperature, and their data are summarized in Table 1. Two intense absorption bands at around 250 nm and 325 nm, as well as a weak low-lying absorption band at 372 nm are observed for the $(dfppy)_2Ir$(Brfl-pic) complex. The two intense absorption bands are assigned to the $\pi-\pi^*$ transitions of the dfppy and Brfl-pic ligand, respectively. The low-lying absorption band is attributed to the spin-allowed singlet metal-to-ligand charge transfer (^{1}MLCT), spin-forbidden triplet metal-to-ligand charge transfer (^{3}MLCT) and $^3\pi-\pi^*$ transitions. Compared to the $(dfppy)_2Ir$(Brfl-pic) complex, the $(dfppy)_2Ir$(Tfl-pic) complex exhibits an increased absorption band from the ancillary ligand at 347 nm and a decreased MLCT absorption band at 410 nm. As the ancillary ligand absorption significantly increases, the MLCT absorption of the $(dfppy)_2Ir$(Tfl-pic) complex becomes much weaker [28].

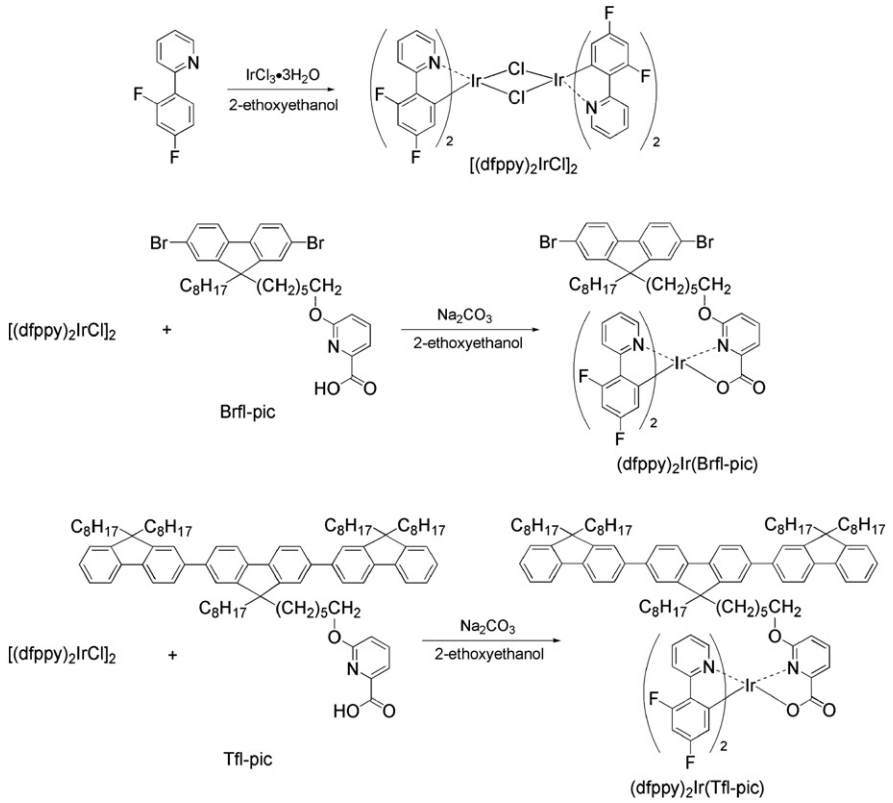

Scheme 1. Synthesis route of the $(dfppy)_2Ir(Brfl\text{-}pic)$ and $(dfppy)_2Ir(Tfl\text{-}pic)$ complexes.

It is interesting that both alkylfluorene-containing iridium (III) complexes exhibit nearly identical PL profiles in DCM solution and their neat films. An intense and structured peak at 471 nm, with an intense shoulder at 498 nm are observed for these two iridium (III) complexes, which is assigned to a blend of ^{1}MLCT and ^{3}MLCT transitions [29]. It implies that introducing a trialkylfluorene or dibromoalkylfluorene unit into picolinic acid has a minor effect on the PL property of their iridium (III) complexes in DCM. In contrast, the PL spectra in neat films exhibit different red-shifted emission for both iridium (III) complexes. However, the introduction of dibromoalkylfluorene and trialkylfluorene groups into iridium (III) complex should induce a better energy transfer which can improve their PL quantum efficiency. The PL quantum yield (Φ_{PL}) was determined to be 0.48 for $(dfppy)_2Ir(Tfl\text{-}pic)$ and 0.43 for $(dfppy)_2Ir(Brfl\text{-}pic)$ in degassed DCM solution at room temperature by using $(dfppy)_2Ir(pic)$ as the standard ($\Phi_{PL} = 0.42$) [30] (Table 1).

3.3. Thermal and dispersible properties

The thermal stability of the two iridium (III) complexes of $(dfppy)_2Ir(Tfl\text{-}pic)$ and $(dfppy)_2Ir(Brfl\text{-}pic)$ was evaluated by thermogravimetric analysis (TGA) under N_2 stream at a scanning rate of 20 °C min^{-1}, and their TGA curves are shown in Fig. S1. The decomposition temperature (T_d) values are 361 °C for $(dfppy)_2Ir(Brfl\text{-}pic)$ and 367 °C for $(dfppy)_2Ir(Tfl\text{-}pic)$, which corresponds to a 5% weight loss. Both iridium (III) complexes present high thermal stability.

In order to make clear their dispersibility in a polymer matrix, the films of two iridium (III) complexes doped with a blend of PBD–PVK at 8 wt% doping concentration were made. Their surface morphologies were recorded by atomic force microscopy (AFM), and the AFM images are shown in Fig. 2. The $(dfppy)_2Ir(Brfl\text{-}pic)$-doped film displays a roughness with $R_a = 0.200$ nm and the $(dfppy)_2Ir(Tfl\text{-}pic)$-doped film exhibits a roughness with $R_a = 0.228$ nm. Both of the iridium (III) complexes exhibit a good dispersibility in the PVK–PBD matrix.

3.4. Electrochemical properties

The electrochemical behavior of the cyclometalated iridium (III) complexes was studied by cyclic voltammetry, and the data are listed in Table 1. Both of the $(dfppy)_2Ir(Brfl\text{-}pic)$ and $(dfppy)_2Ir(Tfl\text{-}pic)$ complexes showed a sole reversible reduction

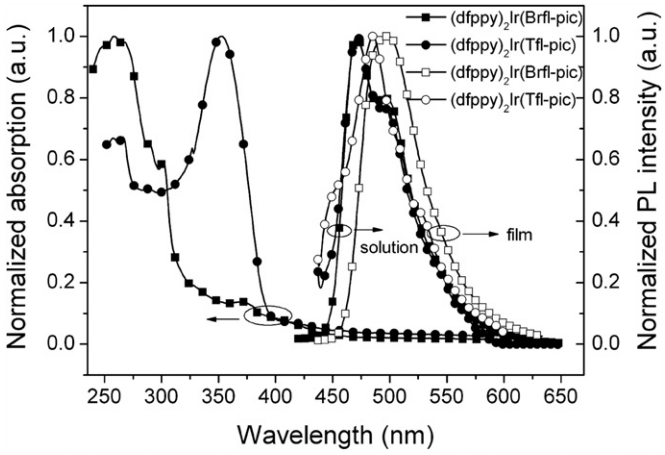

Fig. 1. Normalized UV–vis and PL spectra of the $(dfppy)_2Ir(Brfl\text{-}pic)$ and $(dfppy)_2Ir(Tfl\text{-}pic)$ complexes in DCM and their neat films at room temperature.

Table 1
UV–vis absorption, PL, electrochemical, and thermal properties of $(dfppy)_2Ir(Brfl\text{-}pic)$ and $(dfppy)_2Ir(Tfl\text{-}pic)$.

Compounds	UV–vis/nm	Emission[a]/nm	Emission[b]/nm	Φ_{PL}	E_{red}[c]/mV	HOMO/eV	LUMO/eV	E_g/eV
$(dfppy)_2Ir(Brfl\text{-}pic)$	257, 299 372, 420	471, 498	484	0.43	−1.78	−5.36	−2.56	2.8
$(dfppy)_2Ir(Tfl\text{-}pic)$	252, 325, 345, 418	471, 498	485	0.48	−1.71	−5.54	−2.62	2.92

[a] Measured in DCM at room temperature.
[b] Measured in the neat film at room temperature.
[c] As 10^{-3} M solutions in CH_3CN containing 10^{-1} M NBu_4PF_6 as electrolyte.

wave (E_{red}) at −1.78 V and −1.71 V, respectively. No oxidation waves (E_{ox}) were observed for these iridium (III) complexes. As a result, the E_{ox} has to be calculated by the energy band gap (E_g) and E_{red} according to the formula of $E_{ox} = E_g + E_{red}$, in which E_g is generally estimated from the low-lying absorption edge data. According to the empirical formula of $E_{LUMO} = -(E_{red} + 4.34)$ and $E_{HOMO} = -(E_{ox} + 4.34)$ [31], the highest occupied molecular orbited (HOMO) and the lowest unoccupied molecular orbital (LUMO) energy levels (E_{HOMO} and E_{LUMO}) are calculation to be −5.36 eV and −2.56 eV for the $(dfppy)_2Ir(Brfl\text{-}pic)$ complex, −5.54 eV, and −2.62 eV for the $(dfppy)_2Ir(Tfl\text{-}pic)$ complex, respectively. Introduction of a trialkylfluorene group instead of a dibromoalkylfluorene group is responsible for increasing the energy gap of its iridium (III) complex.

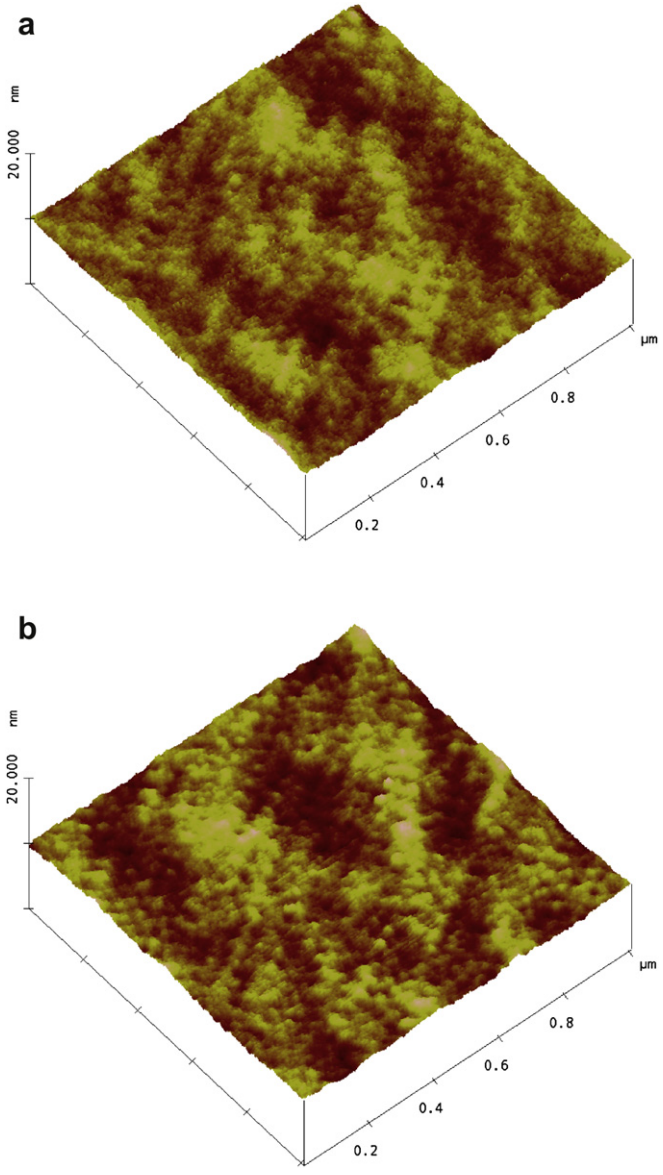

Fig. 2. Atomic force microscope images for: (a) the $(dfppy)_2Ir(Brfl\text{-}pic)$-doped PVK–PBD film; (b) the $(dfppy)_2Ir(Tfl\text{-}pic)$-doped PVK–PBD film. The film thickness was about 80 nm and the dopant concentration was 8 wt%.

3.5. Electroluminescent properties

As $(dfppy)_2Ir(Tfl\text{-}pic)$ exhibited better optophysical and thermal properties than $(dfppy)_2Ir(Brfl\text{-}pic)$, we specially studied the electroluminescent property of $(dfppy)_2Ir(Tfl\text{-}pic)$ in two classes of single-emitting devices (A and B).

Device A doped with 1–8 wt% $(dfppy)_2Ir(Tfl\text{-}pic)$ as the emitting layer was fabricated first, where Ca/Al was used as the cathode. The electroluminescent (EL) spectra of these devices at 13 V are shown in Fig. 3. A maximum emission peak at 475 nm with a shoulder at 430 nm and a longer wavelength band at 570 nm are observed under the given dopant concentrations, in which the 475 nm band is attributed to the iridium (III) complex emission and the 430 nm band is assigned to the PVK emission. The longer wavelength band at 570 nm, more red-shifted compared to its PL profiles, may result from the exciplex emission of iridium (III) complex/PVK + PBD [32]. With increasing dopant concentrations from 1 wt% to 8 wt%, the emission intensity at about 430 nm decreases gradually and that of the longer wavelength band increases gradually. Furthermore, the emission colors have changed from blue to near-white light with increasing dopant concentrations. As shown in Fig. 3, the CIE coordinate diagram displays the emission color located in the near-white light region for the device A at dopant concentrations from 4 wt% to 8 wt%. The current density–voltage–brightness (J–V–B) characteristics of device A is shown in Fig. 4. The luminance

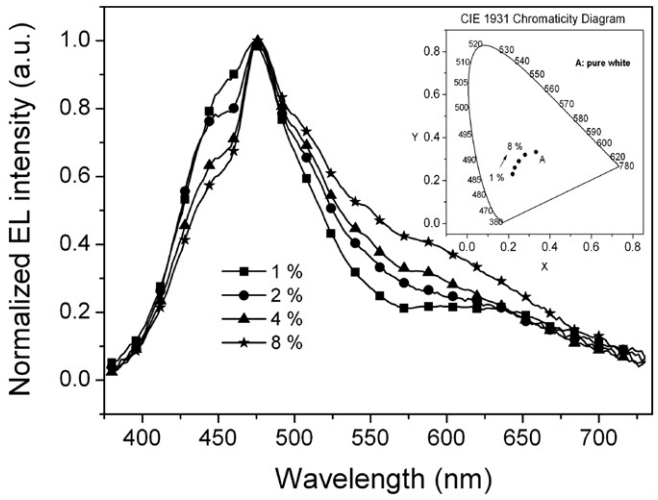

Fig. 3. EL spectra and CIE 1931 chromaticity diagram of the device A at the dopant concentrations from 1 wt% to 8 wt%.

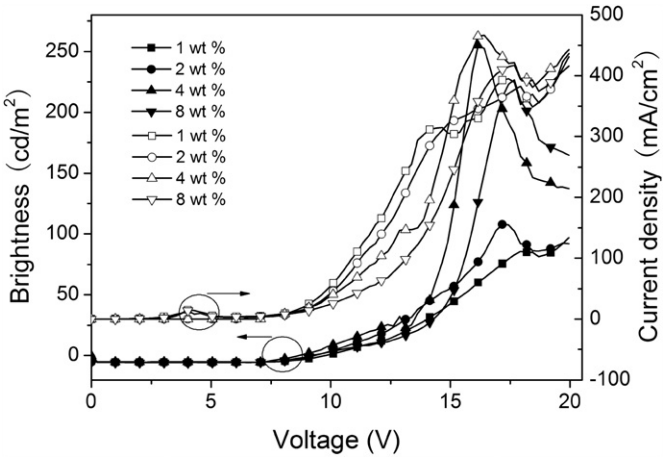

Fig. 4. J–V–B curves of the device A at the dopant concentrations from 1 wt% to 8 wt%.

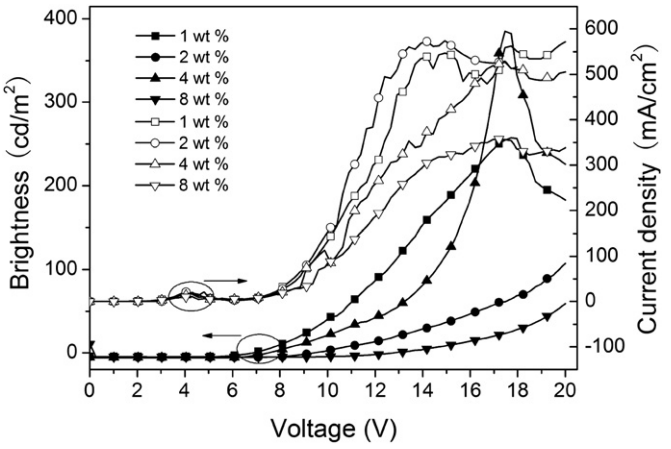

Fig. 6. J–V–B curves of the device B at the dopant concentrations from 1 wt% to 8 wt%.

increases with the increasing dopant concentrations from 1 wt% to 4 wt% and then gradually decreases from 4 wt% to 8 wt%. The highest luminance of 252 cd m^{-2} at 16 V is achieved in device A at 4 wt% doping level. On the other hand, the current density–voltage (J–V) curves show an increasing trend of current density with increasing dopant concentration. These results may imply that the phosphorescent site of $(dfppy)_2Ir(Tfl\text{-}pic)$ serves as a charge trapping site [33].

In order to obtain improved white light, device B was fabricated, where LiF/Al was used as the cathode. The dopant concentrations remained at 1–8 wt%. Fig. 5 shows the EL spectra of device B at 13 V with different dopant concentrations. All EL spectra exhibit a broad emission with three emission peaks at 430 nm, 480 nm and 520 nm, respectively, in which the former is attributed to PVK emission, the second is assigned to the iridium (III) complex emission and the last is attributed to the exciplex emission of iridium (III) complex/PVK + PBD. It is observed that their corresponding CIE coordinates located in near-white light region from (0.26, 0.32) to (0.31, 0.41). The emission intensities at about 430 nm and 520 nm are obviously increased at dopant concentrations of 1–8 wt% compared to the device A, which is the result of the exciton recombination zone has a shift to host matrix because LiF should be enhance the electron transition property [34].

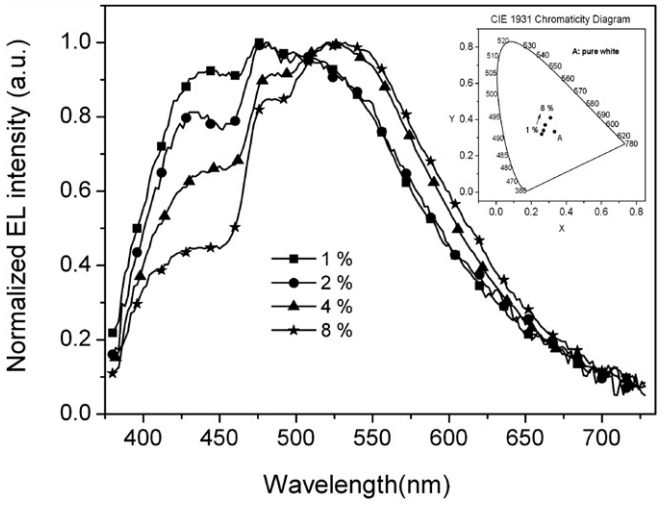

Fig. 5. EL spectra and CIE 1931 chromaticity diagram of the device B at the dopant concentrations from 1 wt% to 8 wt%.

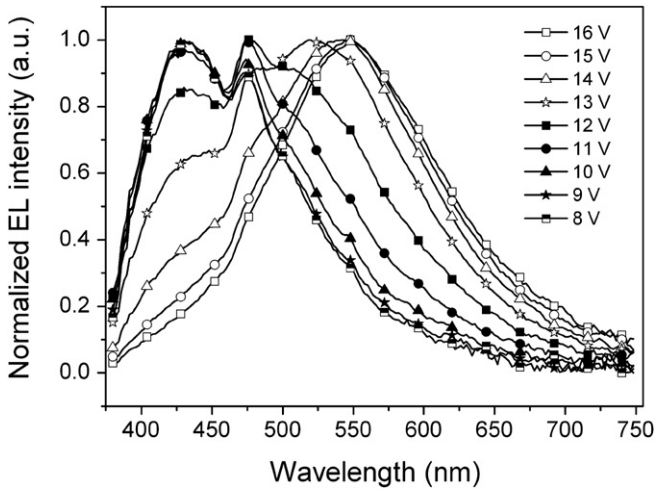

Fig. 7. EL spectra of device B under different applied voltages at a 4 wt% dopant concentrations.

Fig. 6 shows the current density–voltage–brightness (J–V–B) characteristics of device B. The change of luminance and current density versus voltage is identical to that of device A. The maximum luminance of 382 cd m^{-2} (17 V) and a maximum current efficiency of 0.3 cd A^{-1} at J = 97 mA cm^{-2} were obtained in device B at 4 wt% dopant concentration. Device B exhibited higher luminance than device A. It is suggested that the device performance can be improved by tuning the cathode.

To further investigate the white emission based on device B, the EL spectrum under different applied voltages at the dopant concentration of 4 wt% were recorded (Fig. 7). While the applied voltage increased, the emission in the high-energy region is gradually decreased and the emission in the low-energy region grows strong. Accordingly, the color change from the blue to white region and the CIE coordinates varied from (0.19, 0.21) to (0.36, 0.46) (Fig. S2). We presumed that the change of CIE coordinates results from a ratio of exciplex at different applied voltages, which is in accord with a literature report [32].

4. Conclusions

In conclusion, two blue-emitting iridium (II) complexes containing trialkylfluorene picolinic acid derivatives were obtained.

Utilizing the mono-molecular and exciplex emission of the blue-emitting $(dfppy)_2Ir(Tfl\text{-}pic)$ complex, the single-emitting layer devices exhibited near-white emission. By further tuning the cathode, the device presented a more stable white emission. To the best of our knowledge, this is the first report on the application of exciplex emission used an iridium (III) complex as an unitary component in single-emitting layer white PLEDs.

Acknowledgements

Financial support from the National Natural Science Foundation of China (50973093, 20772101 and 20872124), the Science Foundation of Hunan Province (2009FJ2002), the Specialized Research Fund and the New Teachers Fund for the Doctoral Program of Higher Education (20094301110004, 200805301013), the Scientific Research Fund of Hunan Provincial Education Department (10A119), the Open Project Program of Key Laboratory of Environmentally Friendly Chemistry and Applications of Ministry of Education (09HJYH06), and the Postgraduate Science Foundation for Innovation in Hunan Province (CX2009B124).

Appendix. Supplementary data

Supplementary data associated with this article can be found, in the online version, at doi:10.1016/j.dyepig.2011.04.013.

References

[1] Seo JH, Lee SJ, Seo BM, Moon SJ, Lee KH, Park JK, et al. White organic light-emitting diodes showing nearly 100% internal quantum efficiency. Organic Electronics 2010;11:1759–66.
[2] D'Andrade BW, Forrest SR. White organic light-emitting devices for solid-state lighting. Advanced Materials 2004;16:1585–95.
[3] Seo JH, Park JH, Kim YK, Kim JH, Hyung GW, Lee KH, et al. Highly efficient white organic light-emitting diodes using two emitting materials for three primary colors (red, green, and blue). Applied Physics Letters 2007;90:203507–9.
[4] Yook KS, Lee JY. High efficiency and low efficiency roll off in white phosphorescent organic light-emitting diodes by managing host structures. Applied Physics Letters 2008;92:193308–10.
[5] Tong QX, Lai SL, Chan MY, Tang JX, Kwong HL, Lee CS, et al. High-efficiency nondoped white organic light-emitting devices. Applied Physics Letters 2007;91:023503–5.
[6] Ho MH, Hsu SF, Ma JW, Hwang SW, Yeh PC, Chen CH. White p-i-n organic light-emitting devices with high power efficiency and stable color. Applied Physics Letters 2007;91:113518.
[7] Sun Y, Forrest SR. High-efficiency white organic light emitting devices with three separate phosphorescent emission layers. Applied Physics Letters 2007;91:263503–5.
[8] Tsai ML, Liu CY. White light emission from single component polymers fabricated by spin coating. Applied Physics Letters 2003;82:550–2.
[9] Lee YZ, Chen XW, Chen MC, Chen SA. White-light electroluminescence from soluble oxadiazole-containing phenylene vinylene ether-linkage copolymer. Applied Physics Letters 2001;79:308–10.
[10] Huang HH, Chu SY, Kao PC, Chen YC. High efficiency white organic light emitting diodes using rubrene doped N, N′-bis-(1-naphthyl)-N, N′-diphenyl-1,1′-bi-phenyl-4,4′-diamine as an emitting layer. Thin Solid Films 2008;516:5669–72.
[11] Kulkarni AP, Jenekhe SA. Blue–green, orange, and white organic light-emitting diodes based on exciplex electroluminescence of an oligoquinoline acceptor and different hole-transport materials. The Journal of Physical Chemistry C 2008;112:5174–84.
[12] Su HC, Chen HF, Fang FC, Liu CC, Wu CC, Wong KT, et al. Solid-state white light-emitting electrochemical cells using iridium-based cationic transition metal complexes. Journal of the American Chemical Society 2008;130:3413–9.
[13] Yu XM, Kwok HS, Wong WY, Zhou GJ. High-efficiency white organic light-emitting devices based on a highly amorphous iridium(III) orange phosphor. Chemistry of Materials 2006;18:5097–103.
[14] Cocchi M, Kalinowski J, Virgili D, Fattori V, Develay S, Williams JAG. Single-dopant organic white electrophosphorescent diodes with very high efficiency and its reduced current density roll-off. Applied Physics Letters 2007;90:163508–10.
[15] Park YS, Kang JW, Kang DM, Park JW, Kim YH, Kwon SK, et al. Efficient, color stable white organic light-emitting diode based on high energy level yellowish-green dopants. Advanced Materials 2008;20:1957–61.
[16] Kawamura Y, Goushi K, Brooks J, Brown JJ, Sasabe H, Adachi C. 100% phosphorescence quantum efficiency of Ir(III) complexes in organic semiconductor films. Applied Physics Letters 2005;86:071104–6.
[17] Williams EL, Haavisto K, Li J, Jabbour GE. Advanced Materials 2007;19:197;
Tong B, Mei Q, Wang S, Fang Y, Meng Y, Wang B. Nearly 100% internal phosphorescence efficiency in a polymer light-emitting diode using a new iridium complex phosphor. Journal of Materials Chemistry 2008;18:1636–9.
[18] Kim JH, Michelle SL, Alex JKY, Carlson B, Larry RD, Shu CF, et al. Bright red-emitting electrophosphorescent device using osmium complex as a triplet emitter. Applied Physics Letters 2003;83:776–8.
[19] Kalinowski J, Cocchi M, Virgili D, Fattori V, Williams JAG. Mixing of excimer and exciplex emission: a new way to improve white light emitting organic electrophosphorescent diodes. Advanced Materials 2007;19:4000–5.
[20] Zhang GH, Chou HH, Jiang XQ, Sun PP, Cheng CH. Highly efficient white organic light-emitting diodes based on broad excimer emission of iridium complex. Organic Electronics 2010;11:1165–71.
[21] Sun Y, Giebink NC, Kanno H, Ma B, Thompson ME, Forrest SR. Management of singlet and triplet excitons for efficient white organic light-emitting devices. Nature 2006;440:908–12.
[22] Eom SH, Zheng Y, Wrzesniewski E, Lee JI, Chopra N, So F, et al. White phosphorescent organic light-emitting devices with dual triple-doped emissive layers. Applied Physics Letters 2009;94:153303–5.
[23] Wang Q, Ding J, Ma D, Cheng Y, Wang L. Highly efficient single-emitting-layer white organic light-emitting diodes with reduced efficiency roll-off. Applied Physics Letters 2009;94:103503–5.
[24] Kappaun S, Eder S, Sax S, Saf R, Mereiter K, List EJW, et al. WPLEDs prepared from main-chain fluorene-iridium(III) polymers. Journal of Materials Chemistry 2006;16:4389–92.
[25] Jiang J, Jiang C, Yang W, Zhen H, Huang F, Cao Y. High-efficiency electrophosphorescent fluorene-alt-carbazole copolymers N-grafted with cyclometalated Ir complexes. Macromolecules 2005;38:4072–80.
[26] Wang YF, Tang H, Liu Y, Jiang CX, Hu ZY, Zhu MX, et al. Synthesis, optophysics, and electroluminescence of cyclometalated iridium (III) complex with alkyltrifluorene picolinic acid. Tetrahedron 2010;66:1483–8.
[27] Liu Y, Wang YF, Guo HP, Zhu MX, Li C, Peng JB, et al. Synthesis and optoelectronic characterization of a monochromic red-emitting europium (III) complex containing triphenylamine-functionalized phenanthroline. Journal of Physical Chemical C 2011;115:4209–16.
[28] Ragni R, Plummer EA, Brunner K, Hofstraat JW, Babudri F, Farinola GM, et al. Blue emitting iridium complexes: synthesis, photophysics and phosphorescent devices. Journal of Materials Chemistry 2006;16:1161–70.
[29] Xie HZ, Liu MW, Wang OY, Zhang XH, Lee CS, Hung LS, et al. Reduction of self-quenching effect in organic electrophosphorescence emitting devices via the use of sterically hindered spacers in phosphorescence molecules. Advanced Materials 2001;13:1245–8.
[30] You Y, Park SY. Inter-ligand energy transfer and related emission change in the cyclometalated heteroleptic iridium complex: facile and efficient color tuning over the whole visible range by the ancillary ligand structure. Journal of the American Chemical Society 2005;127:12438–9.
[31] Si ZJ, Li J, Li B, Hong ZR, Liu SY, Li WL. Electroluminescence from singlet excited-state of the exciplex between (2,3-dicarbonitrilopyrazino[2,3-f][1,10] phenanthroline)$Re(CO)_3Cl$ and CBP. The Journal of Physical Chemistry C 2008;112:3920–5.
[32] Kolosov D, Adamovich V, Djurovich P, Thompson ME, Adachi C. 1,8-Naphthalimides in phosphorescent organic LEDs: the interplay between dopant, exciplex, and host emission. Journal of the American Chemical Society 2002;124:9945–54.
[33] Hu ZY, Wang YF, Shi DY, Tan H, Zhu WG, Cao Y. Highly-efficiency red-emitting platinum (II) complexes containing 4-diarylamino-1-phenyliso-quinoline ligands in polymer light-emitting diodes: synthesis, structure, photoelectron and electroluminescence. Dyes and Pigments 2010;86:166–73.
[34] Zhong GY, Zhang YQ, Cao XA. Quenching-enhanced shift of recombination zone in phosphorescent organic light-emitting diodes. Organic Electronics 2010;11:1338–43.